

Magnetic structure of two lithium iron phosphates: A- and B- $\text{Li}_3\text{Fe}_2(\text{PO}_4)_3$

G. Rousse^{1,*}, J. Rodriguez-Carvajal², C. Wurm³, C. Masquelier³

¹ Institut Laue-Langevin, BP 156, 38042 Grenoble Cedex 9, France

² Laboratoire Leon Brillouin (CEA-CNRS), CEA/Saclay, 91191 Gif-sur-Yvette Cedex, France

³ Université Picardie Jules Verne, Laboratoire de Reactivité et de Chimie des Solides, 33 rue Saint Leu, 30039 Amiens Cedex France

Received: 18 July 2001/Accepted: 24 October 2001 – © Springer-Verlag 2002

Abstract. The magnetic structures of the monoclinic (P21/n, A-LFP) and rhombohedral (R-3, B-LFP) forms of $\text{Li}_3\text{Fe}_2(\text{PO}_4)_3$ have been determined using neutron powder diffraction at 1.5 K on polycrystalline samples. Magnetic peaks appear in the neutron diffraction patterns below 25 K for both structures, and they can be indexed with a $\mathbf{k} = (000)$ propagation vector. The magnetic moments are found to be collinear and perpendicular to [001] in both structures. The obtained magnetic moments are 4.7 and 3.9 μ_B per iron atom for A-LFP (ferrimagnetic ordering of the two iron sub-lattices) and 4.7 μ_B for the NASICON (B-LFP) form. The Fe atoms are oriented antiparallel within the $[\text{Fe}_2(\text{PO}_4)_3]$ “lantern units”, while there is a parallel orientation of the Fe atoms that do not belong to the same $[\text{Fe}_2(\text{PO}_4)_3]$ lantern unit. The magnetic structure of B-LFP is explained in terms of exchange integrals.

PACS: 75.50.Ee

Three-dimensional polyanionic structures built of interconnected MO_6 octahedra and PO_4 tetrahedra providing an interstitial space partially occupied by alkali cations have been the subject of intense research over the last 20 years, for their unusual ionic conductivity, thermal expansion and electrochemical properties. Of the most widely investigated is the NASICON family $\text{A}_x\text{M}_2(\text{PO}_4)_3$ [1, 2], which offers extensive versatility towards chemical substitutions in the $[\text{M}_2(\text{PO}_4)_3]$ polyanionic framework, into which between 0 and 5 alkali cations may be accommodated. These materials could be used as a cathode for rechargeable lithium batteries.

$\text{Li}_3\text{Fe}_2(\text{PO}_4)_3$ may adopt two distinct crystallographic forms, denoted A-LFP (monoclinic, P21/n) and B-LFP (rhombohedral R-3, NASICON), which differ by the way the $[\text{Fe}_2(\text{PO}_4)_3]$ “lantern units” are connected. The A form is the stable form, prepared via solid state reaction, while the B form is obtained through ion exchange from the NASICON sodium analogue $\text{Na}_3\text{Fe}_2(\text{PO}_4)_3$. In this paper, we discuss the magnetic structure of these two analogs.

1 Experiment

The monoclinic (A-LFP) and rhombohedral (B-LFP) forms of $\text{Li}_3\text{Fe}_2(\text{PO}_4)_3$ were prepared as previously described [3]. Neutron diffraction experiments at 300 K and 1.5 K were performed at the Orphée reactor at the Laboratoire Léon Brillouin in Saclay, France, on the neutron powder diffractometer G4.2 ($\lambda = 2.3433 \text{ \AA}$). The program FullProf [4] was used for crystal-structure refinements using the Rietveld method [5].

2 Magnetic structure of monoclinic A- $\text{Li}_3\text{Fe}_2(\text{PO}_4)_3$

The stable form of $\text{Li}_3\text{Fe}_2(\text{PO}_4)_3$, A-LFP, is monoclinic at room temperature (α -form, space group P21/n). Its crystal structure was previously determined from single-crystal, X-ray diffraction by Bykov et al. [6] and Maksimov et al. [7]. Neutron diffraction patterns recorded when A-LFP is cooled below $T_N = 25 \text{ K}$ show the appearance of some extra reflections. Additionally, the intensity of some peaks already present at high temperature is increased (Fig. 1). All these

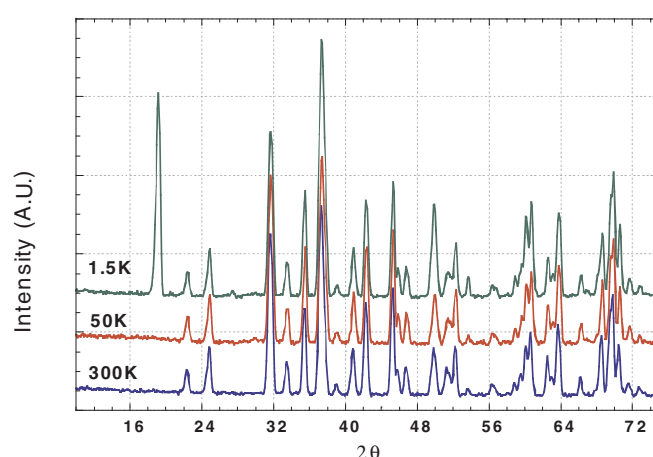


Fig. 1. Neutron diffraction patterns of A-LFP showing the appearance of magnetic peaks at low temperature

*Corresponding author. (Fax: +33-(0)47/620-7648, E-mail: rousse@ill.fr)

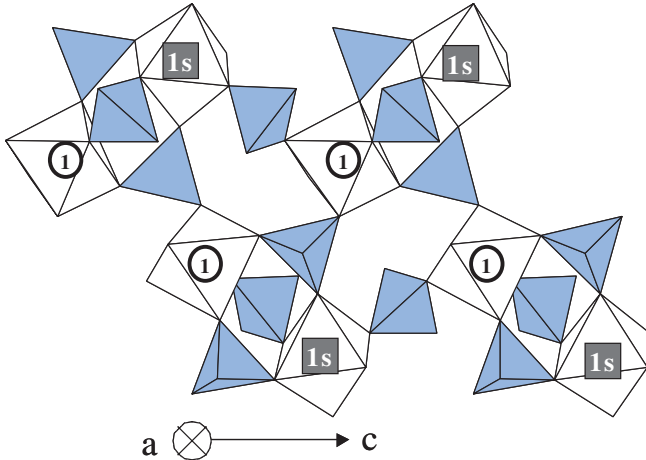


Fig. 2. Representation of the magnetic structure for A-LFP. Solid squares and open circles represent opposite directions of the magnetic moment along [001]

reflections can be indexed with the propagation vector $\mathbf{k} = (000)$, which indicates that the magnetic unit cell is the same as the nuclear unit cell, and, consequently, the space group remains $P21/n$, with lattice parameters $a = 8.5599(2)$ Å, $b = 11.9965(3)$ Å, $c = 8.6096(2)$ Å, and $\gamma = 90.559(2)$. The 8 magnetic Fe^{3+} ions of the cell are distributed on two different crystallographic sites, at general position $4e$ with the following coordinates: for $\text{Fe}(1)$: $x = 0.246$, $y = 0.108$, and $z = 0.462$; and for $\text{Fe}(1s)$: $x = 0.754$, $y = 0.395$, and $z = 0.471$. We determined the magnetic structure using symmetry analysis [8]. Refinement of independent magnetic moments for $\text{Fe}(1)$ and $\text{Fe}(1s)$ led to an antiferromagnetic coupling along the x -axis. Of all the possibilities, the collinear solution $F_X = S_X^1 + S_X^2 + S_X^3 + S_X^4$ ($\Gamma 3$), with opposite magnetic moments for $\text{Fe}(1)$ and $\text{Fe}(1s)$ gives the best agreement between observed and calculated patterns. No component of the magnetic moment exists along the y - and z -directions. We first tried the refinement with an equivalent magnetic moment amplitude for $\text{Fe}(1)$ and $\text{Fe}(1s)$, and at the last stage of the refinement, we allowed the magnetic moments of $\text{Fe}(1)$ and $\text{Fe}(1s)$ to be completely independent. The refined values for the magnetic moment are $4.68(32)$ μ_B for $\text{Fe}(1)$ and $3.96(30)$ μ_B for $\text{Fe}(1s)$, respectively. The structure we found by neutron diffraction confirms experimentally the prediction of Goni et al., the magnetic interaction in each sublattice being ferromagnetic and antiferromagnetically coupled between the two $\text{Fe}(1)$ and $\text{Fe}(1s)$ sublattices [9]. Figure 2 represents the magnetic structure found by neutron diffraction. The solid squares correspond to a negative magnetic moment of $3.96(30)$ μ_B in the x -direction, whereas the open circles correspond to a positive moment of $4.68(32)$ μ_B in the x -direction. In each “lantern unit”, $\text{Fe}(1)$ and $\text{Fe}(1s)$ are antiparallel, whereas two neighbouring lantern units are parallel.

3 Magnetic structure of the NASICON B- $\text{Li}_3\text{Fe}_2(\text{PO}_4)_3$

The rhombohedral B- $\text{Li}_3\text{Fe}_2(\text{PO}_4)_3$ (B-LFP) compound presents the NASICON structure with space group R-3, and its structure was presented in one of our previous papers [3]. Prepared from ion exchange from $\text{Na}_3\text{Fe}_2(\text{PO}_4)_3$, this com-

ound is based on the same $[\text{Fe}_2(\text{PO}_4)_3]$ lantern units as in A-LFP, but the relative positions of these lanterns are different. Although the magnetic properties of the Na analogue B- $\text{Na}_3\text{Fe}_2(\text{PO}_4)_3$ (with a monoclinic $C2/c$ space group) has been widely studied [10], those of B-LFP have scarcely been mentioned, apart from a very recent publication that appeared during the course of our study [11].

As for A-LFP, all the magnetic reflections observed in the neutron diffraction pattern below 25 K can be indexed within the nuclear cell, indicating that the propagation vector for the magnetic structure is $\mathbf{k} = (000)$. The magnetic structure was solved by testing the different basis functions of the irreducible representation for R-3 with $\mathbf{k} = (000)$. There are 2 different crystallographic sites for iron in B-LFP, both in the $6c$ Wyckoff position with atomic coordinates of the atoms within a primitive cell, $(0, 0, z)$ and $(0, 0, -z)$. The structure is very well refined using the collinear model ($F_X(1)$, $F_X(2)$). The values of the magnetic moments of $\text{Fe}(1)$ and $\text{Fe}(2)$ were constrained to be equal; otherwise the refinement leads to an unrealistic value for one of them (over 5 μ_B). The obtained value for $\text{Fe}(1)$ and $\text{Fe}(2)$ is refined to $4.76(3)$ μ_B . The magnetic structure obtained is in agreement with what has been observed for the Na analogues [10]: the two Fe inside the same lantern unit are oriented antiparallel, and the orientation between crystallographically equivalent Fe is parallel (Fig. 3).

To understand the observed magnetic structure in terms of super-super exchange interactions, the same procedure as

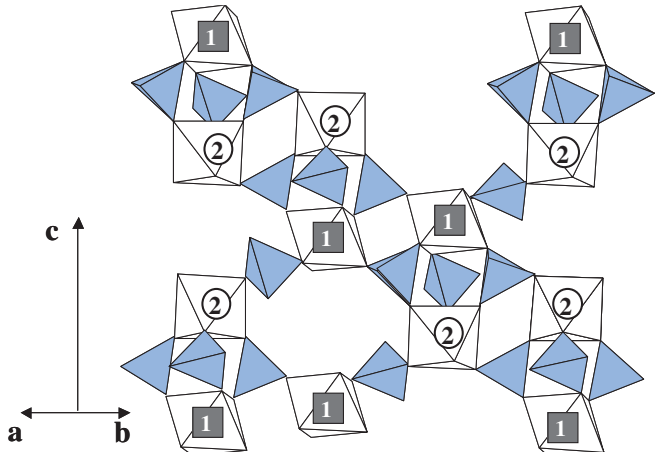


Fig. 3. Representation of the magnetic structure for B-LFP. Solid squares and open circles represent opposite directions of the magnetic moment along [001]

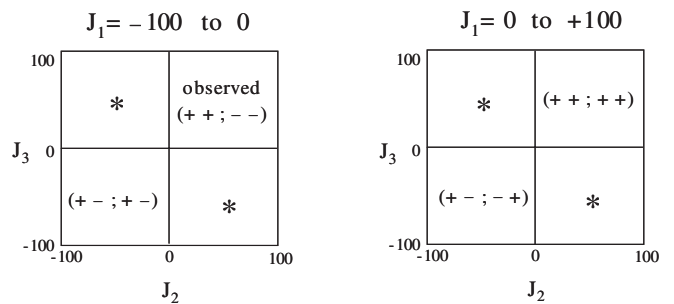


Fig. 4. Magnetic phase diagram for B-LFP. Spin sequences for $\mathbf{k} = (000)$ collinear magnetic structures are indicated. Star: incommensurate or disordered structures

described in [12] was followed. Three exchange paths have to be considered for this structure. J_1 is the shortest one and connects Fe(1) and Fe(2) in the same lantern unit via three equivalent exchange paths involving two oxygen atoms. J_2 connects two Fe(2) atoms, perpendicular to the sheets containing the lantern units. J_3 connects two Fe(2) belonging to two adjacent lantern units. Using numerical calculations, we established phase diagrams with J_1 , J_2 and J_3 as Cartesian axes. In Fig. 4, the calculated magnetic ground state is indicated in each domain. The star indicates domains where incommensurate or disordered structures are found. The observed magnetic structure is $(F_X(1), F_X(2)) = (+; -)$ and is found to be the ground state when $J_1 < 0$ and $J_2 > 0$ and $J_3 > 0$.

4 Conclusion

We solved the magnetic structure of two lithium iron analogs, A-Li₃Fe₂(PO₄)₃ and NASICON B-Li₃Fe₂(PO₄)₃, that differ by the way the [Fe₂(PO₄)₃] lantern units are connected. Both structures are collinear, and in both cases magnetic moments are oriented antiparallel in the same lantern unit. Magnetic phase diagrams, using exchange integrals as Cartesian axes,

are an efficient way to explain and, why not, predict magnetic structures.

References

1. H.Y.P. Hong: Mat. Res. Bull. **11**, 173 (1976)
2. A.K. Padhi, K.S. Nanjundaswamy, J.B. Goodenough: J. Electrochem. Soc. **144**, 1188 (1997)
3. C. Masquelier, A.K. Padhi, K.S. Nanjundaswamy, J.B. Goodenough: J. Solid State Chem. **135**, 228 (1998)
4. J. Rodriguez-Carvajal: Physica B **55**, 192 (1993);
see <http://www.llb.cea.fr/fullweb/powder.htm>
5. H.M. Rietveld: J. Appl. Cryst. **2**, 65 (1969)
6. A.B. Bykov, A.P. Chirkov, L.N. Demyanets, S.N. Doronin, E.A. Genkina, A.K. Ivanov-Shits, I.P. Kondratyuk, B.A. Maksimov, O.K. Mel'nikov, L.N. Muradyan, V.I. Simonov, V.A. Timofeeva: Solid State Ionics **38**, 31 (1990)
7. B.A. Maksimov, L.N. Muradyan, E.A. Genkina, V.I. Simonov: Sov. Phys. Dokl. **31**, 370 (1986)
8. A.S. Wills: J. Appl. Phys. A **74**, this issue (2002)
9. A. Goñi, L. Lezama, N.O. Moreno, L. Fournès, R. Olazcuaga, G.E. Barberis, T. Rojo: Chem. Mater. **12-1**, 62 (2000)
10. N. Fanjat, J.L. Soubeyroux: J. Mag. Magn. Mater. **104**, 933 (1992)
11. A.S. Andersson, B. Kalska, P. Jonsson, L. Haggstrom, P. Nordblad, R. Tellgren, J.O. Thomas: J. Mater. Chem. **10**, 2542 (2000)
12. N. El Khayati, R. Cherkaoui El Moursli, J. Rodriguez-Carvajal, G. Andre, N. Blanchard, F. Bouree, G. Collin, T. Roisnel: Eur. Phys. J. **22**, 429 (2001)